Spin dynamics in the cubic Heisenberg ferromagnet EuS

H. G. Bohn
Institut für Festkörperforschung, Kernforschungsanlage Jülich, D-5170 Jülich, Federal Republic of Germany

A. Kollmar
Institut für Festkörperforschung, Kernforschungsanlage Jülich, D-5170 Jülich, Federal Republic of Germany and Institut Laue-Langevin, 156X, F-38042 Grenoble Cedex, France

W. Zinn
Institut für Festkörperforschung, Kernforschungsanlage Jülich, D-5170 Jülich, Federal Republic of Germany
(Received 2 July 1984)

Using the inelastic-neutron-scattering technique, we have undertaken an extensive study of the spin dynamics in EuS. The experiments were performed on a ^{153}EuS single crystal with the scattering vector $\vec{q}$ along the [100] direction. The q values extended over the range between 0.11 and 1.06 Å^{-1}, and the temperatures ranged from 1.2 to 50 K ($=3T_c$). It was found that spin-wave renormalization theory holds well up to $0.8T_c$. For temperatures above T_c and up to the highest temperatures of our experiments, the line shapes are well described by the recently developed correlation theories. From the q dependence of the linewidth of the dynamical response at $T=T_c$, a dynamical scaling exponent $z=2.09(6)$ was deduced. The deviation from the pure Heisenberg value of $z=\frac{5}{2}$ is attributed to the dipolar interactions.

I. INTRODUCTION

Among the few examples of insulating ferromagnetic systems, the europium compounds EuO and EuS are of particular interest since they are model substances for cubic isotropic Heisenberg ferromagnets.[1] Both have the NaCl structure and the magnetism is due to the well-localized $4f$ electrons. The divalent europium forms an S-state ion with a stable moment of $7\mu_B$ (spin $S=\frac{7}{2}$), and there are only minor solid-state effects, as can be seen from spin-density measurements.[2]

It was recognized rather early that the exchange interactions reach at least next-nearest neighbors (NNN).[3] This has recently been confirmed by inelastic-neutron-scattering experiments for the case of EuS,[4] and both for EuO and EuS the exchange parameters J_1 to nearest neighbors (NN) and J_2 to NNN have been determined with high precision from spin-wave-dispersion measurements.[4–6] Although the basic parameters of these systems are now well known there still remain some problems in the understanding of fundamental thermodynamic properties, as for instance the temperature dependence of the spontaneous magnetization as measured by NMR.[4,7,8] Thus it is tempting to test the underlying spin-wave theories by studying the temperature dependence of the spin-wave excitations.

Additionally, much interest has recently focused on the spin dynamics of itinerant magnetic systems around and above the ordering temperature T_c. The bulk of the recent experimental and theoretical work has been devoted to the question of whether or not there exist magnonlike excitations in the paramagnetic phase of the metallic ferromagnets Fe and Ni.[9] For comparison, it is interesting to study the behavior of a typical Heisenberg system such as EuS.

Apart from this, EuS is interesting in itself for two reasons. There are competing exchange interactions J_1 and J_2, and the magnitude of the dipolar energy is comparable to the exchange energy.[8] Both are expected to influence the spin dynamics of the system.

In this paper we report the results of an extensive neutron scattering investigation of the spin dynamics of EuS. Preliminary results for a limited wave vector and temperature range have already been published.[10] The measurements have been extended to temperatures between $0.1T_c$ and $3T_c$ and wave vectors covering the full first Brillouin zone in the [100] direction. We will discuss the renormalization of magnon energies and line broadening due to magnon-magnon interactions below T_c, the linewidth at T_c which gives the dynamical scaling exponent z, and the line shapes above T_c. The latter will be compared to recent theories which apply to the paramagnetic state of Heisenberg ferromagnets.

II. EXPERIMENTAL DETAILS

Though it is well known that neutron scattering is a powerful tool for investigating magnetic properties on a microscopic scale, this method has only been applied in a few cases to the europium chalcogenides.[2,4–6,10] The reason is that natural europium, being composed of 52 at.% ^{153}Eu and 48 at.% ^{151}Eu, is highly absorptive for thermal neutrons. Thus, at least for inelastic scattering experiments, material enriched in the less-absorbant ^{153}Eu isotope has to be used. We have used the same mosaic-type single crystal, enriched to 99.2% in the ^{153}Eu isotope,

which was already used in our determination of the exchange parameters from the low-temperature spin-wave dispersion.[4] Details of the sample preparation and shape of the sample can be found in Ref. 4. It should be noted that it is extremely important to perform the experiments on single crystals since in contrast to EuO the spin-wave dispersion is strongly anisotropic. This is due to the competing exchange interactions in EuS, and would give rise to severe line broadening in powdered samples for larger wave vectors.

The neutron scattering experiments were performed at the high-flux reactor of the Institut Laue-Langevin, Grenoble using the triple-axis spectrometers IN2 and IN12 at a thermal beamport and the cold source, respectively. Incoming neutron energies of 3.21, 1.12, and 0.78 THz were used depending on whether high energy resolution or intensity was more important. Graphite or beryllium filters were placed in the primary beam in order to remove higher order contamination. The spectrometers were operated in the constant-q mode with fixed incoming neutron energy. The temperature was measured by means of a calibrated carbon resistor glued to the sample holder. From the intensity of the critical scattering, the ordering temperature T_c was found to be 16.6 ± 0.1 K in accordance with the result from an independent hysteresis measurement.[11] The value is characteristic for stoichiometric EuS.

All of the neutron scattering measurements were made around the (000) reciprocal lattice point, i.e., in the forward direction which gives the highest intensity due to the $4f$ magnetic form factor.[2] We have checked that a measurement around (200) gives only a reduction of the signal-to-noise ratio. The scattering vector $\vec{Q}=\vec{k}_i-\vec{k}_f=\vec{G}_{000}+\vec{q}=\vec{q}$, where $\vec{k}_i$ and $\vec{k}_f$ are the wave vectors of the incoming and scattered neutrons, respectively, was directed along the [100] direction for two reasons. Firstly, the spin-wave energies are highest in this direction which makes them more easily accessible to experiment, and secondly, there is a well-defined angle $\theta_{\vec{q}}$ between $\vec{q}$ and the magnetization even in a multidomain sample with no external field applied. Since $\langle 111\rangle$ is the easy axis for the magnetization $\vec{M}$ in EuS,[12] this angle is always $\pm54.7°$, irrespective of the actual domain. Thus line-broadening effects due to multidomain scattering are avoided, as only $\sin^2\theta_{\vec{q}}$ enters into the dispersion law [see Eq. (8)] and thus into the scattering cross section.[13]

The lattice parameter of EuS being $a_0=5.95$ Å at low temperatures we cover the full first Brillouin zone in the [100] direction with scattering vectors up to 1.06 Å^{-1}. One of the main experimental difficulties was the determination of the background scattering near zero energy transfer. This is very important for temperatures close to and above T_c since then the magnetic scattering is concentrated in this energy regime. We have carefully measured the temperature and q dependence of the scattering from the cryostat and the empty sample holder. Unfortunately, it was impossible to determine precisely the contribution from the ceramic glue which was used to fix the mosaic pieces of the sample. Also, even with the isotopically enriched EuS considerable absorption corrections had to be applied. Table I gives the relative transmission for the various incoming neutron energies used. These values, of course, vary slightly during a constant-q scan. After correcting our spectra for these background contributions a temperature- and q-independent part due to incoherent elastic nuclear scattering from the EuS remained. As demonstrated in Fig. 1, this is well separated from the inelastic magnon scattering at temperatures $T\ll T_c$ and can be fitted by an extra Gaussian with a linewidth determined by instrumental resolution, which could then be subtracted from all the spectra in the next

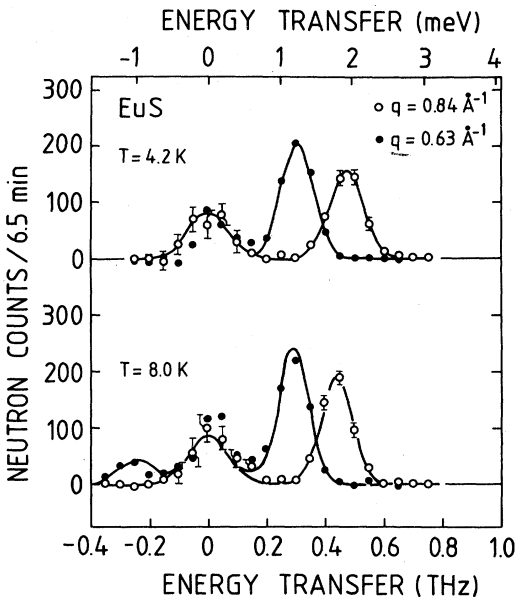

FIG. 1. Typical inelastic-neutron-scattering spectra of EuS at 4.2 and 8 K for two different scattering vectors q. Note the temperature- and wave-vector-independent nuclear incoherent elastic scattering. The points are the measured intensities with the background subtracted, while the solid lines represent the best fits to the data of two Gaussian functions. For $q=0.84$ Å^{-1}, error bars are also given.

TABLE I. Transmission of the ^{153}EuS sample and instrumental resolution (as determined from the incoherent scattering of vanadium) for various incoming neutron energies E_i used in the experiments. For convenience, k_i is also given.

E_i (THz)	k_i (Å^{-1})	Transmission (%)	Resolution FWHM (THz)	Instrument
3.31	2.572	71	0.161	IN2
1.13	1.500	56	0.035	IN12
0.78	1.250	51	0.018	IN12

step of the data-reduction process.

From this discussion it is clear that data points around zero energy transfer could only be obtained with relatively large experimental uncertainties. The width of this regime is determined by the instrumental resolution. In Table I we also give the resolution as determined from the incoherent scattering of a vanadium sample.

Finally, it should be noted that the experiments were made in three independent runs with similar but not identical spectrometer configurations. Thus the scatter of the results is also an indication of the reproduciblity of the data.

III. EXPERIMENTAL RESULTS AND COMPARISON WITH THEORY

The neutron cross section for the scattering from a magnetic sample is given by[13]

$$\frac{d^2\sigma}{d\omega\, d\Omega}=A\frac{k_f}{k_i}\frac{\hbar\omega/k_BT}{1-\exp(-\hbar\omega/k_BT)}\frac{\chi(\vec{q})}{\chi_0}F(\vec{q},\omega)\ , \tag{1}$$

where

$$\hbar\omega=E_i-E_f \tag{2}$$

denotes the energy change of the neutron due to the scattering. The coefficient A contains the magnetic form factor which is close to unity for the q range of our experiments[2] and a number of trivial constants. $\chi(\vec{q})/\chi_0$ is the wave-vector-dependent susceptibility normalized to that of the noninteracting spin system. In this paper we are mainly interested in the behavior of the normalized spectral weight or relaxation function $F(\vec{q},\omega)$ since, for the case of EuS, $\chi(\vec{q})$ is determined more directly and thus with more precision from double-axis experiments.[14] The question of whether both longitudinal and transversal parts contribute significantly to the scattering and the related problem of the analytical form of $F(\vec{q},\omega)$ is discussed in great detail in Ref. 14. Since also in the case of EuS there was no extra scattering intensity to be found near $\omega=0$ within the accuracy of the measurement, we decided to take for the spectral weight function at $T<T_c$ a double Lorentzian

$$F(\vec{q},\omega)=\frac{\Gamma/2}{2\pi\hbar}\times\left[\frac{1}{(\Gamma/2)^2+(\omega-\omega_{\vec{q}})^2}+\frac{1}{(\Gamma/2)^2+(\omega+\omega_{\vec{q}})^2}\right], \tag{3}$$

in accordance with many other experiments. This function is peaked at the magnon energy, i.e., $\pm\hbar\omega_{\vec{q}}$ corresponding to spin-wave creation and annihilation, respectively, and has a linewidth $\hbar\Gamma$ [full width at half maximum (FWHM)]. These two parameters were the essential results of fitting Eqs. (1) and (3), folded with the instrumental resolution, to our measured spectra. The shape of $F(\vec{q},\omega)$ for $T>T_c$ will be discussed in Sec. III D.

A. Spin-wave renormalization

Spin-wave theory is well developed for the case of isotropic Heisenberg systems such as EuS.[15] The exchange Hamiltonian $\hat{\mathscr{H}}_{mn}$ between two localized spins $\vec{S}_m$ and $\vec{S}_n$ of magnitude S at lattice sites $\vec{R}_m$ and $\vec{R}_n$, respectively, is given by

$$\hat{\mathscr{H}}_{mn}=-2J_{mn}\vec{S}_n\cdot\vec{S}_m\ , \tag{4}$$

where J_{mn} is the exchange parameter depending only on the distance $r=|\vec{R}_m-\vec{R}_n|$. The low-temperature excitations of this system are the well-known spin waves, which follow the dispersion relation

$$\hbar\omega^{\rm ex}_{\vec{q}}=E^{\rm ex}_{\vec{q}}=2S[J(0)-J(\vec{q})]\ , \tag{5}$$

where

$$J(\vec{q})=\sum_{\vec{r}}J_{mn}e^{i\vec{q}\cdot\vec{r}}=\sum_i z_iJ_i\gamma^i_{\vec{q}}\ . \tag{6}$$

J_i describes the isotropic exchange interaction of an Eu^{2+} ion with its z_i neighbors of the ith-neighbor shell, and the lattice sums

$$\gamma^i_{\vec{q}}=\frac{1}{z_i}\sum_{n=1}^{z_i}e^{i\vec{q}\cdot\vec{r}_n} \tag{7}$$

are easily calculated for a fcc lattice.

In the case of EuS, the dipolar interactions have also to be taken into account. Then the Holstein-Primakoff spin-wave theory applies:[16]

$$\hbar\omega_{\vec{q}}=[E^{\rm ex}_{\vec{q}}(E^{\rm ex}_{\vec{q}}+2A_{\vec{q}})]^{1/2} \tag{8}$$

with $A_{\vec{q}}=\frac{1}{2}g\mu_B\mu_0M(T)\sin^2\theta_{\vec{q}}$. Here $\theta_{\vec{q}}$ denotes the angle between the direction of spontaneous magnetization $\vec{M}$ and the scattering vector $\vec{q}$. As discussed above, $\sin^2\theta_{\vec{q}}=\frac{2}{3}$ for the geometry used in our experiments.

From the analysis of the low-temperature spin-wave dispersion, the exchange parameters of EuS have been obtained in an earlier paper.[4] At finite temperatures magnon-magnon interactions begin to play a role, which influences both the spin-wave energies and the linewidth of the neutron inelastic scattering.

For the dispersion it can be shown[17,18] that it is still of the form of Eq. (8) if one replaces J_i by

$$J_i(T)=J_i[1-C_i(T)/S]\ , \tag{9}$$

where

$$C_i(T)=\frac{1}{N}\sum_{\vec{q}}(1-\gamma^i_{\vec{q}})n_{\vec{q}}\ , \tag{10}$$

and

$$n_{\vec{q}}=[\exp(\hbar\omega_{\vec{q}}/k_BT)-1]^{-1} \tag{11}$$

is the thermal population factor. If the dispersion is known the magnetization $M=M(T)$ is calculated from[16,19]

$$\frac{M_0-M(T)}{M_0}=\frac{1}{NS}\sum_{\vec{q}}\frac{A_{\vec{q}}}{\hbar\omega_{\vec{q}}}n_{\vec{q}}+\frac{1}{2NS}\sum_{\vec{q}}\left[\frac{A_{\vec{q}}}{\hbar\omega_{\vec{q}}}-1\right]. \tag{12}$$

$\mu_0 M_0=1.53$ T is the magnetization for complete spin parallelism. Obviously, Eqs. (8)—(12) have to be solved self-consistently.

The summations were carried out by exact numerical integration over the first Brillouin zone (BZ). From the given set of EuS exchange parameters $J_1,\ldots,J_5$ both the renormalized magnon energies and the renormalized values of $J_i(T)$ are derived for any given temperature without further assumptions. It turned out that the self-consistent calculation procedure failed to converge above $0.99T_c$ thereby giving a good indirect estimate of T_c. It should be noted that this large range of validity is rather surprising in view of the various approximations made in the theoretical treatments.

In Fig. 2 we have plotted the renormalization of the two most important exchange constants $J_1(T)$ and $J_2(T)$ as calculated from the theory.

An experimental check of the predictions of the spin-wave renormalization theory is provided by measuring the temperature dependence of the magnon energies. Typical spectra for $q=0.84$ Å^{-1}, corrected for background as discussed above, are shown in Fig. 3. The peak shift toward smaller magnon energy with increasing temperature is clearly seen. The solid lines represent the best fit to the data where up to 10 K we have used a Gaussian line-shape function since in this temperature range the linewidth is determined by the instrumental resolution. For higher temperatures up to T_c, Eq. (3) was convoluted with the known spectrometer resolution. The behavior of the dynamical response in the paramagnetic phase will be discussed in Sec. III D. From the spectra at 12 and 15.9 K one might infer that there is some extra scattering intensity near zero energy transfer. However, looking at the relatively large error bars due to the heavy corrections which had to be applied to these data points we feel that this should not be taken seriously. Thus within experimental uncertainty there is no indication of longitudinal fluctuations contributing to the scattering which should give a peak at $\omega=0$ according to theory.[20]

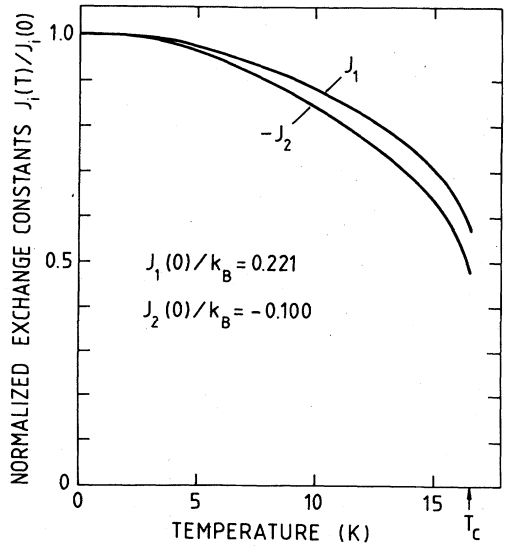

FIG. 2. Calculated renormalization of the NN and NNN exchange parameters J_1 and J_2 of EuS.

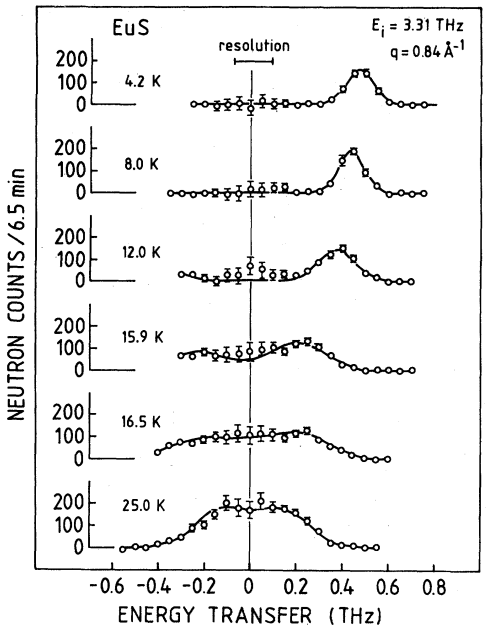

FIG. 3. Triple-axis scans in EuS for temperatures below and above $T_c=16.6$ K. The points are measured intensities with background and nuclear incoherent elastic scattering subtracted. The solid lines represent the best fits to the data of the spectral weight function appropriate for the corresponding temperature (see discussion in text). The instrumental resolution is also indicated. Note that there is no extra scattering intensity observed near zero energy transfer, indicating that there is no extra spectral weight associated with a central diffusive peak.

We have carried out these measurements for the temperature range $1.2<T<T_c=16.6$ K and q values covering the full first Brillouin zone. The results are summarized in numeric form in Table II and shown in Fig. 4 where we have plotted the magnon energies versus temperature for six different q values. All data which were collected during the three experimental runs are given. Error bars which are due to statistical errors are plotted when they are larger than the symbols used.

The solid lines are calculated from the spin-wave-renormalization theory outlined above with no adjustable parameter except for the exchange constants $J_1,\ldots,J_5$ which were determined from the low-temperature spin-wave dispersion. This means that the energies for $T=0$ are fixed.

The q dependence of the renormalization is known to be small for EuO,[21] and in fact it has been shown explicitly for a cubic ferromagnet with NN exchange only that the ratio $\omega_{\vec{q}}(T)/\omega_{\vec{q}}(T=0)$ is independent of q.[22] In Fig. 5 we have plotted this ratio versus temperature which is only a different way of presenting the data of Fig. 4. The calculated temperature dependence falls within the shaded

TABLE II. Magnon energies $\hbar\omega_{\vec{q}}$ in EuS for various temperatures T and wave vectors q along the [100] direction. The energy and wave vectors of the incident neutron are also given.

k_i (Å^{-1})	E_i (THz)	T (K)	q (Å^{-1})	$\hbar\omega_{\vec{q}}$ (THz)	k_i (Å^{-1})	E_i (THz)	T (K)	q (Å^{-1})	$\hbar\omega_{\vec{q}}$ (THz)
1.500	1.13	4.1	0.21	0.052(2)	1.500	1.13	14.1	0.63	0.229(2)
1.250	0.78	4.1	0.21	0.047(2)	1.500	1.13	15.6	0.63	0.171(5)
1.800	1.62	4.2	0.21	0.055(27)	2.572	3.31	15.9	0.63	0.120(8)
1.250	0.78	7.0	0.21	0.040(2)	1.500	1.13	16.5	0.63	0.125(5)
1.250	0.78	10.0	0.21	0.037(2)	2.572	3.31	16.5	0.63	0.110(6)
1.250	0.78	12.0	0.21	0.033(2)	2.572	3.31	1.3	0.84	0.491(2)
1.250	0.78	14.1	0.21	0.028(2)	2.572	3.31	2.2	0.84	0.486(4)
1.250	0.78	16.0	0.21	0.012(2)	2.572	3.31	4.2	0.84	0.474(2)
1.250	0.78	16.5	0.21	0.006(2)	2.572	3.31	6.0	0.84	0.462(2)
2.572	3.31	1.3	0.32	0.074(2)	2.572	3.31	8.0	0.84	0.442(2)
1.500	1.13	4.1	0.32	0.087(3)	2.572	3.31	8.0	0.84	0.434(12)
2.572	3.31	4.2	0.32	0.079(2)	2.572	3.31	10.0	0.84	0.427(3)
1.250	0.78	7.1	0.32	0.080(2)	1.500	1.13	12.0	0.84	0.403(5)
2.572	3.31	7.1	0.32	0.083(2)	2.572	3.31	12.0	0.84	0.380(20)
1.250	0.78	10.0	0.32	0.074(2)	2.572	3.31	12.0	0.84	0.378(4)
1.250	0.78	12.0	0.32	0.068(2)	2.572	3.31	14.0	0.84	0.322(10)
1.500	1.13	14.1	0.32	0.056(2)	1.500	1.13	14.1	0.84	0.367(7)
1.250	0.78	16.0	0.32	0.030(2)	1.500	1.13	15.6	0.84	0.283(19)
1.250	0.78	16.5	0.32	0.018(2)	2.572	3.31	15.9	0.84	0.219(11)
1.500	1.13	4.1	0.42	0.147(2)	2.572	3.31	16.0	0.84	0.278(40)
2.572	3.31	4.2	0.42	0.138(2)	1.500	1.13	16.5	0.84	0.237(11)
2.572	3.31	4.2	0.42	0.147(5)	2.572	3.31	16.6	0.84	0.190(10)
2.572	3.31	6.0	0.42	0.142(3)	2.572	3.31	1.3	1.06	0.554(2)
1.250	0.78	7.1	0.42	0.136(2)	2.572	3.31	2.2	1.06	0.553(5)
2.572	3.31	8.0	0.42	0.138(2)	2.572	3.31	4.2	1.06	0.543(2)
1.250	0.78	10.0	0.42	0.129(3)	2.572	3.31	4.2	1.06	0.538(2)
1.250	0.78	12.0	0.42	0.117(2)	2.572	3.31	6.0	1.06	0.536(10)
2.572	3.31	12.0	0.42	0.114(5)	2.572	3.31	8.0	1.06	0.520(7)
2.572	3.31	12.0	0.42	0.109(3)	2.572	3.31	8.0	1.06	0.498(8)
1.250	0.78	14.1	0.42	0.093(2)	2.572	3.31	10.0	1.06	0.486(15)
1.500	1.13	15.6	0.42	0.068(3)	1.500	1.13	12.0	1.06	0.458(7)
1.250	0.78	16.0	0.42	0.056(2)	2.572	3.31	12.0	1.06	0.452(6)
2.572	3.31	1.3	0.63	0.319(7)	2.572	3.31	12.0	1.06	0.432(12)
2.572	3.31	2.2	0.63	0.311(6)	2.572	3.31	14.0	1.06	0.360(10)
2.572	3.31	4.2	0.63	0.306(2)	1.500	1.13	14.1	1.06	0.424(4)
2.572	3.31	4.2	0.63	0.310(7)	1.500	1.13	15.6	1.06	0.385(26)
2.572	3.31	6.0	0.63	0.300(2)	2.572	3.31	15.9	1.06	0.280(8)
2.572	3.31	8.0	0.63	0.291(7)	2.572	3.31	16.0	1.06	0.317(18)
2.572	3.31	10.0	0.63	0.271(3)	1.500	1.13	16.5	1.06	0.328(46)
2.572	3.31	12.0	0.63	0.239(5)	2.572	3.31	16.5	1.06	0.276(10)
1.500	1.13	12.0	0.63	0.252(2)	2.572	3.31	16.6	1.06	0.268(32)
2.572	3.31	14.0	0.63	0.182(11)					

region for all wave vectors. Thus also for EuS the theoretical q dependence is much smaller than the scatter of the experimental data. This scatter is partly due to the statistical errors mentioned above; however, mainly it is due to the fact that the data were taken in several independent runs and normalized to the same set of extrapolated energies $E(0)=\hbar\omega_{\vec{q}}(T=0)$. Slight changes in the spectrometer calibration may then produce such scatter, especially for low energies. The deviations from theory are more pronounced for small q values, a result which has already been pointed out by Keffer and Loudon,[18] who showed that small-q spin waves should renormalize more severely than those of larger q.

From these experimental results we conclude that the spin-wave-renormalization theory which takes into account Dyson's dynamical interaction between pairs of magnons[17] is valid up to about 13.5 K, i.e., $T/T_c \approx 0.8$ in the case of EuS. During the preliminary analysis of our data we found a considerably smaller range of validity of the renormalization theory.[4,10] This, however, was based on only a few measurements which happened to deviate from theory all in the same direction, and must be considered accidental with respect to the comprehensive set of experimental results available now.

Finally we wish to note that the intensity of the magnon scattering is experimentally found to vary as T/q^2 to within $\pm 10\%$, which is expected from Eq. (1) [$\chi(\vec{q})/\chi_0 \propto T/q^2$ for $T \ll T_c$].

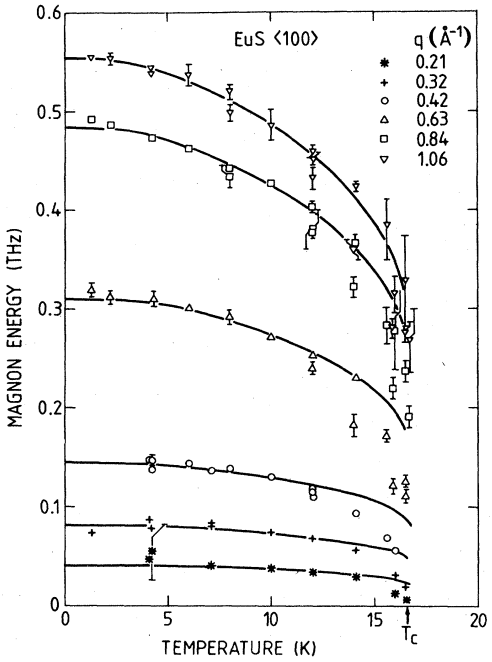

FIG. 4. Renormalization of spin-wave energies in EuS. The solid lines are calculated using the same theory which leads to the temperature variation of the exchange constants shown in Fig. 2. Only the exchange constants determined from the low-temperature spin-wave dispersion enter into this theory as parameters.

B. Spin-wave damping

Up to now we have dealt only with the peak shift of the neutron spectra. As is readily seen from Fig. 3 the spin-wave excitations become heavily damped when T approaches T_c. This is primarily due to magnon-magnon interactions. The limited instrumental resolution allowed these effects to be observable only above 10 K, i.e., for $T/T_c > 0.6$.

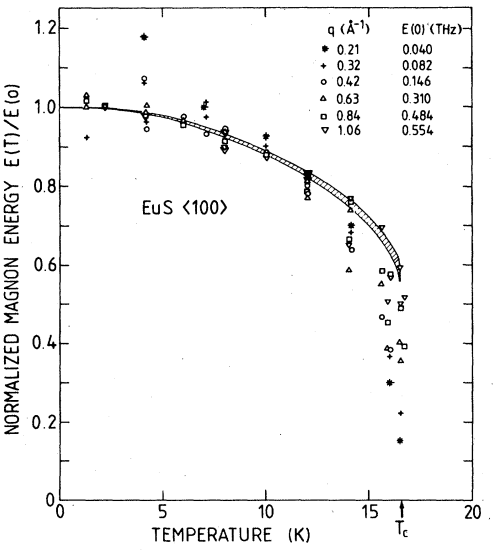

FIG. 5. Temperature variation of the magnon energies for various wave vectors relative to their values at low temperature. The data points are the same as in Fig. 4. This plot demonstrates that there is only little q dependence in the magnon renormalization. The calculations for all q values fall within the shaded regime.

Unfortunately the existing theories of the damping of spins waves[20,23] are not very well worked out in the q-ω regime of our experiments. The linewidth Γ should vary like

$$\Gamma \propto \begin{cases} q^4 \ln^2(k_B T/\hbar\omega_{\vec{q}}), & \hbar\omega_{\vec{q}} \ll k_B T \quad (13a) \\ q^3, & \hbar\omega_{\vec{q}} \gg k_B T\,. \quad (13b) \end{cases}$$

Additionally, the formulas are only derived in the limit $(a_0 q)^2 \ll 1$. In our measurements the data cover the $a_0 q$ range $0.63 < a_0 q < 6.3$. The most complete set of data was taken at $T = 14.1$ K, where the spectra were measured for small q with an incoming neutron energy of 1.12 THz and for large q with $E_i = 3.31$ THz, respectively (see Table III). At this temperature the condition $\hbar\omega_{\vec{q}} = k_B T$ is fulfilled at about $q = 0.7$ Å^{-1}.

In Fig. 6 we have plotted the observed linewidth versus wave vector on a double-logarithmic scale. For comparison lines corresponding to $\Gamma \propto q^4$ and $\Gamma \propto q^3$ are also drawn. Though the quality of the data does not allow for a quantitative analysis there is obviously a transition region around $\hbar\omega_{\vec{q}} = k_B T$. At this point $\Gamma(q)$ vanishes, actually, according to Eq. (13a). Both more resolved theories and more experimental data are required if one wishes to get a detailed understanding of the spin-wave damping in EuS in this regime.

In conclusion of Secs. III A and III B, we state that spin-wave theory gives an excellent description of the behavior of the Heisenberg system EuS up to $T/T_c \approx 0.8$ as far as neutron scattering experiments are concerned. As noted above, there still remains a discrepancy to magnetization data as measured by NMR. From the results of our detailed analysis of the spin-wave behavior of EuS at elevated temperature we conclude that the solution to this question should be reached within the NMR analysis itself.

C. Linewidth at T_c

A special set of experiments was devoted to the wave-vector dependence of the linewidth at T_c as from this type of measurement the dynamical scaling exponent z can be derived. As discussed by Hohenberg and Halperin,[24] for a purely exchange coupled three-dimensional isotropic Heisenberg system $z = \frac{5}{2}$ is expected, whereas for dipolar

TABLE III. Linewidth $\hbar\Gamma$ (FWHM) of EuS at $T = 14.1$ K.

E_i (THz)	q (Å^{-1})	$\hbar\Gamma$ (THz)
0.78	0.21	0.009(1)
1.13	0.32	0.015(11)
0.78	0.42	0.062(8)
1.13	0.63	0.065(12)
1.13	0.84	0.103(30)
1.13	0.95	0.208(43)

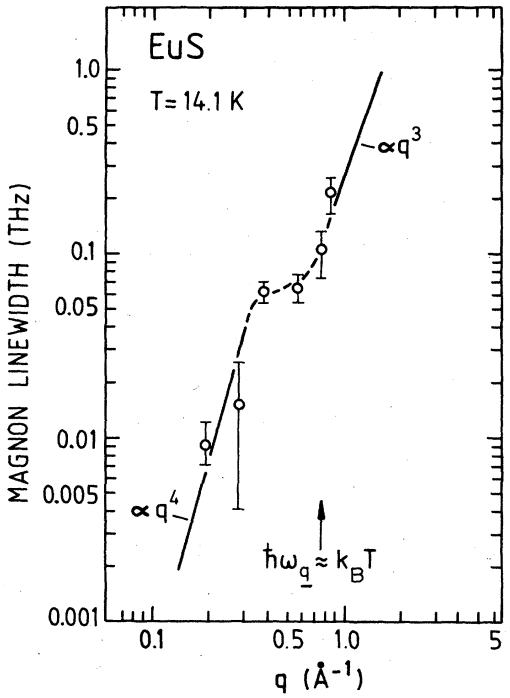

FIG. 6. Linewidth (FWHM) of the spin-wave excitations in EuS versus wave vector q at $T=14.1$ K. The solid line is only a guide to the eye. The straight parts of the curve in this double-logarithmic plot are meant to indicate a slope proportional to q^3 or q^4, respectively. The change in slope occurs near $q\approx 0.7$ Å^{-1}, where $\hbar\omega_{\vec{q}}=k_BT$ approximately holds.

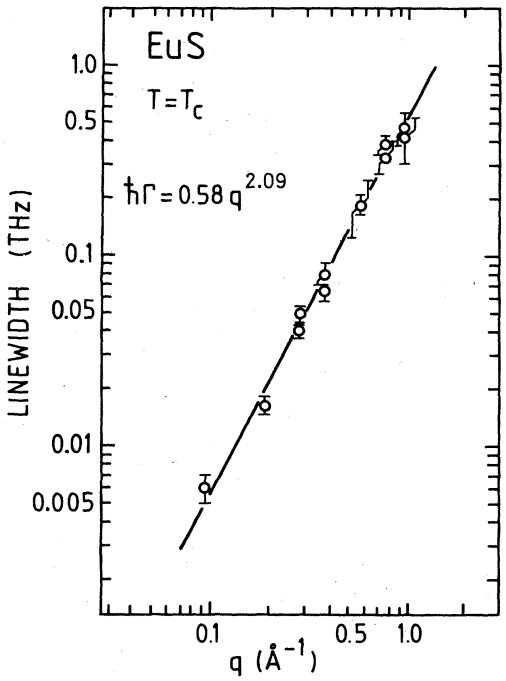

FIG. 7. Linewidth at T_c versus q. The straight line represents the best fit to the data. From the slope a dynamical scaling exponent of $z=2.09(6)$ is derived.

systems $z\approx 2$ applies. The linewidth observed in the neutron scattering experiment is given by

$$\Gamma(q;T=T_c)\propto q^z\,. \tag{14}$$

The value of z to be obtained depends also on the q range covered by the experimental technique. For example, for EuO a crossover from $z=2.04$ at $q\approx 0$ to $z=2.29$ for $0.12<q<0.48$ Å^{-1} was observed.[14,25] This has been attributed to the dipolar forces which are not negligible even in EuO and which contribute mainly at large wavelengths.[26] Similar behavior was also found for Fe and Ni.[27]

Our measurements on EuS were performed for $0.1<q<1.06$ Å^{-1}. The data were analyzed in the same way as for $T<T_c$, though for $q=0.1$ Å^{-1}, Eq. (3) collapses into a single Lorentzian centered at $\omega=0$. The resulting linewidths (FWHM) are summarized in Table IV. They are plotted versus q on a double-logarithmic scale in Fig. 7. Obviously the data are well described by the simple power law

$$\Gamma(q,T_c)=(0.58\pm 0.04)q^{2.09\pm 0.06}\ \text{THz}\,. \tag{15}$$

This dynamical critical exponent $z=2.09$ is even closer to the dipolar value of 2 than it is for EuO. This fact, however, is not surprising since the ratio between the dipolar and the exchange energy in EuS is larger than in EuO by a factor of 2.6.

ESR measurements yielded $z=1.88(6)$ in the case of EuS.[28] However, no indication of dipolar crossover is found from our experiments though the estimated dipolar crossover wave vector $q_d^{\text{EuS}}=1.72q_d^{\text{EuO}}=0.27$ Å^{-1} (Refs. 25, 27, and 29) lies just within the q range of our measurement. Instead an average value is observed by the neutron scattering experiment.

Finally it should be noted that due to the different critical exponents z for EuO and EuS there is no evidence for a constant relation between the corresponding linewidths for all q. Thus the relation

$$\frac{\Gamma^{\text{EuO}}(q,T_c)}{\Gamma^{\text{EuS}}(q,T_c)}=\left[\frac{a_0^{\text{EuS}}}{a_0^{\text{EuO}}}\right]^{5/2}\frac{T_c^{\text{EuO}}}{T_c^{\text{EuS}}}=2.9 \tag{16}$$

as predicted in Refs. 30 and 31 is only a rough approximation. Actually it varies between 1.8 at $q=0.11$ Å^{-1} and 3 at $q=1.06$ Å^{-1} from the comparison of our data on EuS with those reported for EuO in Ref. 14.

TABLE IV. Linewidth $\hbar\Gamma$ (FWHM) of EuS at T_c.

E_i (THz)	q (Å^{-1})	$\hbar\Gamma$ (THz)
0.78	0.11	0.006(1)
0.78	0.21	0.017(1)
		0.016(1)
0.78	0.32	0.040(3)
		0.049(4)
0.78	0.42	0.079(12)
		0.063(6)
1.13	0.63	0.186(20)
		0.188(63)
1.13	0.84	0.384(43)
		0.334(64)
1.13	1.06	0.420(121)
		0.467(87)

D. Line shapes above T_c

Recent experimental interest has focused on the spin dynamics in the paramagnetic state of isotropic ferromagnets. In this context mainly the metallic band ferromagnets Fe, Co, and Ni have been investigated[9,32,33] with efforts directed towards the main question of whether spin diffusion provides a satisfactory description of the neutron data[33] or whether there are relevant deviations due to spin-wave-like excitations.[34]

Thus it is interesting to look at the behavior of an ideal Heisenberg system. This has been done for the case of EuO where for q at the boundary of the first BZ, and at temperatures up to $2T_c$ rather well-defined peaks were found in constant-q scans.[6] The isomorphic system EuS is even more interesting due to its competing exchange interactions $J_1>0$ and $J_2<0$ which result in a higher degree of magnetic short-range order as expressed by the NN correlation function.[35] These recently developed detailed theories of the paramagnetic state of EuO and EuS also predict a considerable change in the line shape when going from EuO to EuS.[35,36] These effects should show up most clearly in the [111] direction where there are no spin-wave-like peaks at all to be expected from the theoretical calculations. Unfortunately, our experiments on EuS were performed before these detailed theories were published, so all of our data points were taken along the [100] direction for experimental convenience as discussed in Sec. II.

For $T>T_c$ we have taken two sets of measurements with incoming neutron energies of 3.31 and 1.13 THz, respectively. The spectra were analyzed using the shape function given in Ref. 36,

$$F(\vec{q},\omega)=\frac{1}{\pi}\frac{\tau\delta_1\delta_2}{[\omega\tau(\omega^2-\delta_1-\delta_2)]^2+(\omega^2-\delta_1)^2}\ , \tag{17}$$

with

$$\delta_1=\langle\omega^2\rangle_{\vec{q}},\quad \delta_1\delta_2=\langle(\omega^2-\langle\omega^2\rangle_{\vec{q}})^2\rangle_{\vec{q}}\ ,$$

$$\tau=(\pi\delta_2/2)^{-1/2}\ ,$$

where $\langle\omega^2\rangle_{\vec{q}}$ and $\langle\omega^4\rangle_{\vec{q}}$ are the second and fourth frequency moments of F. For simplicity we have taken this analytical form of the line shape though the essential features are also within Lindgard's work.[35] We have calculated

$$\chi(\vec{q})/\chi_0=2\frac{(T/T_c)^{\gamma}}{[(a_0\kappa_1)^2+(a_0q)^2]^{1-\eta/2}}$$

by using the values for the exponents γ and η and the inverse correlation length κ_1 as given in the literature.[37] Thus, only δ_1 and δ_2 had to be determined from the least-squares fitting of Eqs. (1) and (17) to the neutron spectra, while the overall normalization constant A could be kept fixed for each set of measurements.

Typical line shapes as measured at 18 K ($1.08T_c$), 25 K ($1.5T_c$), and 50 K ($3T_c$) for $q=0.63$ Å^{-1}, 0.84 Å^{-1}, and 1.05 Å^{-1} are shown in Fig. 8. There is obviously no

TABLE V. Results from the least-squares fits of Eq. (17) to the EuS spectra for $T>T_c$.

E_i (THz)	T (K)	T/T_c	q (Å^{-1})	δ_1 (K^2)	δ_2 (K^2)
3.31	17.0	1.02	1.06	151	164
3.31	17.0	1.02	0.84	120	156
3.31	17.5	1.05	1.06	141	220
3.31	17.5	1.05	0.84	120	251
3.31	18.0	1.08	1.06	132	146
1.13	18.0	1.08	1.06	125	165
1.13	18.0	1.08	0.95	138	169
1.13	18.0	1.08	0.84	118	140
3.31	18.0	1.08	0.84	107	223
1.13	18.0	1.08	0.74	87	165
1.13	18.0	1.08	0.63	33	82
3.31	19.0	1.14	1.06	133	159
3.31	19.0	1.14	0.84	119	309
1.13	20.1	1.21	0.84	113	140
3.31	25.0	1.51	1.06	94	160
1.13	25.0	1.51	1.06	94	120
3.31	25.0	1.51	0.84	71	158
1.13	25.0	1.51	0.84	75	110
1.13	25.0	1.51	0.63	30	90
3.31	36.0	2.17	1.06	77	99
3.31	36.0	2.17	0.84	61	140
3.31	36.0	2.17	0.63	31	89
1.13	50.0	3.00	1.06	58	139
1.13	50.0	3.00	0.84	40	122
1.13	50.0	3.00	0.63	28	91

well-resolved peak in the magnetic response. Instead for $q \gtrsim 0.74$ Å^{-1} the line shape gets a clear shoulder. Maybe one should not speak of "spin waves" for such broad features as we have done in a preliminary analysis of the data[10] since it has been demonstrated theoretically that the equations of motion of the spin system can give rise to such a behavior which in turn may be enhanced by short-range magnetic ordering.[36] The solid lines represent the best fit to the data using Eq. (17) with the indicated values of δ_1 and δ_2, expressed in units of K^2 for a more convenient comparison to the theoretical results of Ref. 36. In Table V we have collected all the δ_1 and δ_2 which have been deduced from our measurements in the paramagnetic state of EuS and in Fig. 9(a) we have plotted δ_1 versus T/T_c for three q values. The solid lines represent smooth interpolations to our data points. In order to compare our experimental results with the theoretical results of Ref. 36, which were obtained at $T/T_c = 1.25$ and 1.75, respectively, we have taken our interpolated values at these temperatures (solid symbols), and in Fig. 9(b) we have plotted them together with the results from the calculations (open circles) versus wave vector q. The solid lines are guides for the eye, and they demonstrate the perfect agreement between theory and experiment for $q \geq 0.63$ Å^{-1} at $T = 1.25T_c$ and $T = 1.75T_c$, respectively. For the parameter δ_2, which is very sensitive to small energy transfer, the agreement is not quite as good. However, this should not be overstressed since at small ω the data are taken with relatively large experimental errors for reasons discussed above.

A few spectra were also measured at small q. In this regime the line shape becomes essentially Lorentzian, showing spin-diffusion behavior. It should be noted, however, that Eq. (17) is equally as capable of fitting these spectra if $\delta_1 \ll \delta_2$. Here no quantitative analysis has been performed, since we have undertaken only a few unsystematic measurements so far.

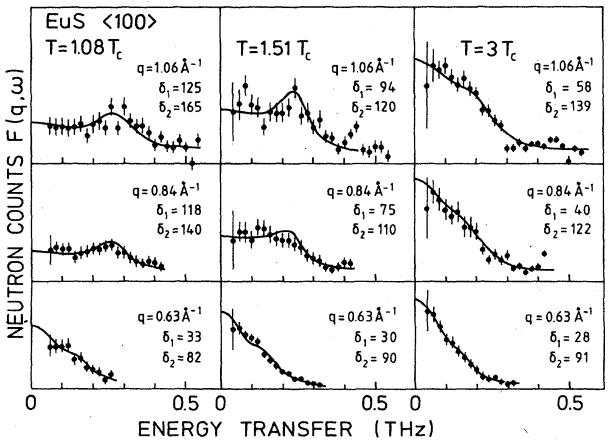

FIG. 8. Shape function $F(\vec{q},\omega)$ for EuS above T_c. Incoming neutron energy was $E_i = 1.13$ THz. Thus no correction for instrumental resolution is needed. The solid lines represent the best fit of Eq. (17) to the experimental data. The resulting parameters δ_1 and δ_2 are given.

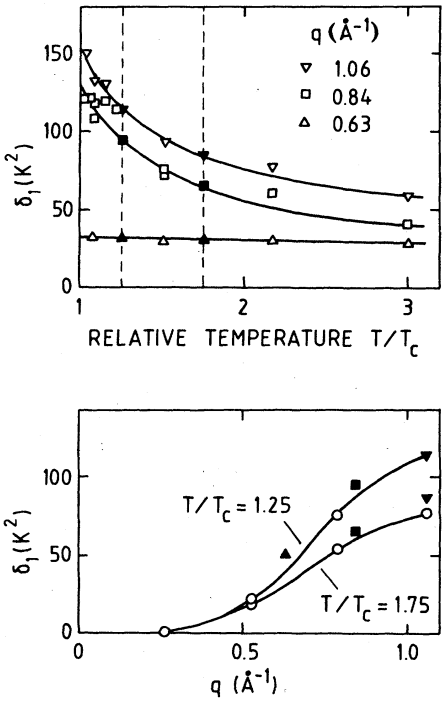

FIG. 9. Second moment δ_1 of $F(\vec{q},\omega)$ in units of K^2 in EuS for $T > T_c$ and various wave vectors. The solid lines are smooth interpolations to the measured data points. For comparison with theory the interpolated values at $T/T_c = 1.25$ and 1.75, respectively, are taken (solid symbols) and plotted in the lower half of the figure together with the theoretical results (○) versus q.

In conclusion, our results confirm that the recently developed theories provide a quantitative description of the existing experiments on the spin dynamics in the paramagnetic state of EuS and EuO.

IV. SUMMARY

We have undertaken a comprehensive study of the temperature dependence of the spin dynamics in the Heisenberg model system EuS by means of inelastic neutron scattering. The measurements were performed on a single crystal along the [100] direction. The magnon energies are found to be well described by Dyson's renormalization theory[17] up to $T/T_c = 0.8$. For $T > 0.6T_c$ spin-wave damping is observed which shows an anomaly in the linewidth if $\hbar\omega_{\vec{q}} \approx k_B T$.

From the wave-vector dependence of the linewidth at T_c the dynamical critical scaling exponent z is deduced to be 2.09(6). The deviation from the value $z = \frac{5}{2}$ expected for a purely exchange-coupled Heisenberg system is attributed to the dipolar interactions which are known to be important in EuS. The dipolar crossover wave vector is estimated to be about 0.27 Å^{-1} in this sytem, hence it lies within the q range of our experiments.

The line shape in the paramagnetic state is perfectly ex-

plained by recent theories[35,36] for all wave vectors and temperatures up to $3T_c$. At large q it gets a clear shoulder at an energy corresponding to about half the magnon energy at low temperature. The position of this spin-wave-like peak is only weakly temperature dependent. The interesting theoretical prediction that no such spin-wave-like peak in the [111] direction should show up has not yet been tested and must await further experiments.

ACKNOWLEDGMENTS

It is a pleasure to thank Dr. B. Dorner (Institut Laue-Langevin), Professor H. Capellmann (Rheinisch Westfälische Technische Hockschule, Aachen), and Dr. P. A. Lindgard (Risø National Laboratory) for helpful and stimulating discussions on the experimental and theoretical aspects of our measurements.

[1]See, e.g., P. Wachter, in *Handbook of the Physics and Chemistry of Rare Earths,* edited by K. A. Gschneidner and L. Eyring (North-Holland, Amsterdam, 1979), Vol. 2, Chap. 19; W. Zinn, J. Magn. Magn. Mater. **3**, 23 (1976), and references therein.

[2]J. W. Cable and W. C. Koehler, J. Magn. Magn. Mater. **5**, 258 (1977); H. G. Bohn, W. Zinn, and F. Tasset, J. Phys. (Paris) Colloq. **43**, C7-141 (1982).

[3]T. R. McGuire, B. E. Argyle, M. W. Shafer, and J. S. Smart, J. Appl. Phys. **34**, 1345 (1963); J. Callaway and D. C. McCollum, Phys. Rev. **130**, 1741 (1963).

[4]H. G. Bohn, W. Zinn, B. Dorner, and A. Kollmar, Phys. Rev. B **22**, 5447 (1980).

[5]L. Passell, O. W. Dietrich, and J. Als-Nielsen, Phys. Rev. B **14**, 4897 (1976).

[6]H. A. Mook, Phys. Rev. Lett. **46**, 508 (1981).

[7]M. Neusser, H. Lütgemeier, and W. Zinn, J. Magn. Magn. Mater. **4**, 42 (1977); O. W. Dietrich, A. J. Henderson, and H. Meyer, Phys. Rev. B **12**, 2844 (1975).

[8]S. H. Charap and E. L. Boyd, Phys. Rev. **133**, A811 (1964).

[9]See, e.g., J. P. Wicksted, G. Shirane, and O. Steinsvoll, Phys. Rev. B **29**, 488 (1984), and references therein.

[10]H. G. Bohn, W. Zinn, B. Dorner, and A. Kollmar, J. Appl. Phys. **52**, 2228 (1981).

[11]B. Saftić, private communication.

[12]G. E. Everett and R. A. Ketcham, J. Phys. (Paris) Colloq. **32**, C 1-545 (1971).

[13]W. Marshall and S. W. Lovesey, *Theory of Thermal Neutron Scattering* (Oxford University Press, London, 1971).

[14]O. W. Dietrich, J. Als-Nielsen, and L. Passell, Phys. Rev. B **14**, 4923 (1976).

[15]F. Keffer, in *Encyclopedia of Physics,* edited by H. P. J. Wijn (Springer, Berlin, 1966), Vol. XVIII/2.

[16]T. Holstein and H. Primakoff, Phys. Rev. **58**, 1098 (1940).

[17]F. J. Dyson, Phys. Rev. **102**, 1217 (1956); **102**, 1230 (1956); W. Marshall and S. W. Lovesey, *Theory of Thermal Neutron Scattering,* Ref. 13, pp. 264–267.

[18]F. Keffer and R. Loudon, J. Appl. Phys. Suppl. **32**, 2S (1961).

[19]P. K. Schwob, M. Tachiki, and G. E. Everett, Phys. Rev. B **10**, 165 (1974).

[20]V. G. Vaks, A. I. Larkin, and S. A. Pikin, Zh. Eksp. Teor. Fiz. **53**, 1089 (1967) [Sov. Phys.—JETP **26**, 647 (1968)].

[21]C. J. Glinka, V. J. Minkiewicz, L. Passell, and M. W. Shafer, in *Magnetism and Magnetic Materials—1973 (Boston),* proceedings of the 19th Annual Conference on Magnetism and Magnetic Materials, edited by C. D. Graham and J. J. Rhyne (AIP, New York, 1974), p. 1060.

[22]M. Bloch, Phys. Rev. Lett. **9**, 286 (1962).

[23]A. B. Harris, Phys. Rev. **175**, 674 (1968); **184**, 606 (1969).

[24]P. C. Hohenberg and B. I. Halperin, Rev. Mod. Phys. **49**, 435 (1977).

[25]R. A. Dunlap and A. M. Gottlieb, Phys. Rev. B **22**, 3422 (1980); J. Kötzler, W. Scheithe, R. Blickhan, and E. Kaldis, Solid State Commun. **26**, 641 (1978).

[26]For a recent discussion, see J. Kötzler, Phys. Rev. Lett. **51**, 833 (1983).

[27]C. Hohenemser, L. Chow, and R. M. Suter, Phys. Rev. B **26**, 5056 (1982).

[28]J. Kötzler, G. Kamleiter, and G. Weber, J. Phys. C **9**, L361 (1976).

[29]D. L. Huber, J. Phys. Chem. Solids **32**, 2145 (1971).

[30]E. K. Riedel, J. Appl. Phys. **42**, 1383 (1971).

[31]J. Hubbard, J. Phys. C **4**, 53 (1971).

[32]J. W. Lynn, Phys. Rev. B **11**, 2624 (1975); **28**, 6550 (1983); C. J. Glinka, V. J. Minkiewicz, and L. Passell, *ibid.* **16**, 4084 (1977); O. Steinsvoll, C. F. Majkrzak, G. Shirane, and J. Wicksted, Phys. Rev. Lett. **51**, 300 (1983).

[33]Y. J. Uemura, G. Shirane, O. Steinsvoll, and J. Wicksted, Phys. Rev. Lett. **51**, 2322 (1983).

[34]J. W. Lynn, Phys. Rev. Lett. **52**, 775 (1984).

[35]P. A. Lindgard, Phys. Rev. B **27**, 2980 (1983).

[36]A. P. Young and B. S. Shastry, J. Phys. C **15**, 4547 (1982).

[37]J. Als-Nielsen, O. W. Dietrich, and L. Passell, Phys. Rev. B **14**, 4908 (1976).